

# Observation of $B^- \rightarrow J/\psi \Lambda \bar{p}$ and Searches for $B^- \rightarrow J/\psi \Sigma^0 \bar{p}$ and $B^0 \rightarrow J/\psi p \bar{p}$ Decays

Q. L. Xie,<sup>8</sup> K. Abe,<sup>6</sup> K. Abe,<sup>39</sup> I. Adachi,<sup>6</sup> H. Aihara,<sup>41</sup> Y. Asano,<sup>45</sup> T. Aushev,<sup>10</sup> S. Bahinipati,<sup>4</sup> A. M. Bakich,<sup>36</sup> E. Barberio,<sup>17</sup> M. Barbero,<sup>5</sup> I. Bedny,<sup>1</sup> U. Bitenc,<sup>11</sup> I. Bizjak,<sup>11</sup> S. Blyth,<sup>20</sup> A. Bondar,<sup>1</sup> A. Bozek,<sup>23</sup> M. Bračko,<sup>6,16,11</sup> J. Brodzicka,<sup>23</sup> T. E. Browder,<sup>5</sup> Y. Chao,<sup>22</sup> A. Chen,<sup>20</sup> W. T. Chen,<sup>20</sup> B. G. Cheon,<sup>3</sup> R. Chistov,<sup>10</sup> Y. Choi,<sup>35</sup> A. Chuvikov,<sup>31</sup> S. Cole,<sup>36</sup> J. Dalseno,<sup>17</sup> M. Danilov,<sup>10</sup> M. Dash,<sup>46</sup> L. Y. Dong,<sup>8</sup> A. Drutskoy,<sup>4</sup> S. Eidelman,<sup>1</sup> Y. Enari,<sup>18</sup> S. Fratina,<sup>11</sup> N. Gabyshev,<sup>1</sup> T. Gershon,<sup>6</sup> A. Go,<sup>20</sup> G. Gokhroo,<sup>37</sup> B. Golob,<sup>15,11</sup> A. Gorišek,<sup>11</sup> J. Haba,<sup>6</sup> K. Hayasaka,<sup>18</sup> H. Hayashii,<sup>19</sup> M. Hazumi,<sup>6</sup> L. Hinz,<sup>14</sup> T. Hokuue,<sup>18</sup> Y. Hoshi,<sup>39</sup> S. Hou,<sup>20</sup> W.-S. Hou,<sup>22</sup> Y. B. Hsiung,<sup>22</sup> T. Iijima,<sup>18</sup> K. Ikado,<sup>18</sup> A. Imoto,<sup>19</sup> A. Ishikawa,<sup>6</sup> R. Itoh,<sup>6</sup> M. Iwasaki,<sup>41</sup> Y. Iwasaki,<sup>6</sup> J. H. Kang,<sup>47</sup> J. S. Kang,<sup>13</sup> P. Kapusta,<sup>23</sup> S. U. Kataoka,<sup>19</sup> N. Katayama,<sup>6</sup> H. Kawai,<sup>2</sup> T. Kawasaki,<sup>25</sup> H. R. Khan,<sup>42</sup> H. Kichimi,<sup>6</sup> J. H. Kim,<sup>35</sup> S. M. Kim,<sup>35</sup> K. Kinoshita,<sup>4</sup> P. Krokovny,<sup>1</sup> C. C. Kuo,<sup>20</sup> Y.-J. Kwon,<sup>47</sup> G. Leder,<sup>9</sup> S. E. Lee,<sup>33</sup> T. Lesiak,<sup>23</sup> J. Li,<sup>32</sup> D. Liventsev,<sup>10</sup> F. Mandl,<sup>9</sup> T. Matsumoto,<sup>43</sup> A. Matyja,<sup>23</sup> W. Mitaroff,<sup>9</sup> K. Miyabayashi,<sup>19</sup> H. Miyake,<sup>28</sup> H. Miyata,<sup>25</sup> Y. Miyazaki,<sup>18</sup> R. Mizuk,<sup>10</sup> G. R. Moloney,<sup>17</sup> T. Nagamine,<sup>40</sup> Y. Nagasaka,<sup>7</sup> E. Nakano,<sup>27</sup> Z. Natkaniec,<sup>23</sup> S. Nishida,<sup>6</sup> O. Nitoh,<sup>44</sup> T. Nozaki,<sup>6</sup> S. Ogawa,<sup>38</sup> T. Ohshima,<sup>18</sup> S. Okuno,<sup>12</sup> S. L. Olsen,<sup>5</sup> Y. Onuki,<sup>25</sup> W. Ostrowicz,<sup>23</sup> H. Ozaki,<sup>6</sup> P. Pakhlov,<sup>10</sup> H. Palka,<sup>23</sup> C. W. Park,<sup>35</sup> N. Parslow,<sup>36</sup> R. Pestotnik,<sup>11</sup> L. E. Pilonen,<sup>46</sup> Y. Sakai,<sup>6</sup> N. Satoyama,<sup>34</sup> K. Sayeed,<sup>4</sup> O. Schneider,<sup>14</sup> M. E. Sevier,<sup>17</sup> H. Shibuya,<sup>38</sup> B. Schwartz,<sup>1</sup> V. Sidorov,<sup>1</sup> A. Somov,<sup>4</sup> N. Soni,<sup>29</sup> S. Stanič,<sup>26</sup> M. Starič,<sup>11</sup> K. Sumisawa,<sup>28</sup> T. Sumiyoshi,<sup>43</sup> F. Takasaki,<sup>6</sup> K. Tamai,<sup>6</sup> M. Tanaka,<sup>6</sup> Y. Teramoto,<sup>27</sup> X. C. Tian,<sup>30</sup> K. Trabelsi,<sup>5</sup> T. Tsuboyama,<sup>6</sup> T. Tsukamoto,<sup>6</sup> S. Uehara,<sup>6</sup> T. Uglov,<sup>10</sup> Y. Unno,<sup>6</sup> S. Uno,<sup>6</sup> P. Urquijo,<sup>17</sup> G. Varner,<sup>5</sup> K. E. Varvell,<sup>36</sup> S. Villa,<sup>14</sup> C. H. Wang,<sup>21</sup> M.-Z. Wang,<sup>22</sup> Y. Watanabe,<sup>42</sup> E. Won,<sup>13</sup> A. Yamaguchi,<sup>40</sup> Y. Yamashita,<sup>24</sup> M. Yamauchi,<sup>6</sup> J. Ying,<sup>30</sup> Y. Yuan,<sup>8</sup> S. L. Zang,<sup>8</sup> C. C. Zhang,<sup>8</sup> J. Zhang,<sup>6</sup> L. M. Zhang,<sup>32</sup> Z. P. Zhang,<sup>32</sup> V. Zhilich,<sup>1</sup> and T. Ziegler<sup>31</sup>

(The Belle Collaboration)

<sup>1</sup>*Budker Institute of Nuclear Physics, Novosibirsk*

<sup>2</sup>*Chiba University, Chiba*

<sup>3</sup>*Chonnam National University, Kwangju*

<sup>4</sup>*University of Cincinnati, Cincinnati, Ohio 45221*

<sup>5</sup>*University of Hawaii, Honolulu, Hawaii 96822*

<sup>6</sup>*High Energy Accelerator Research Organization (KEK), Tsukuba*

<sup>7</sup>*Hiroshima Institute of Technology, Hiroshima*

<sup>8</sup>*Institute of High Energy Physics, Chinese Academy of Sciences, Beijing*

<sup>9</sup>*Institute of High Energy Physics, Vienna*

<sup>10</sup>*Institute for Theoretical and Experimental Physics, Moscow*

<sup>11</sup>*J. Stefan Institute, Ljubljana*

<sup>12</sup>*Kanagawa University, Yokohama*

<sup>13</sup>*Korea University, Seoul*

<sup>14</sup>*Swiss Federal Institute of Technology of Lausanne, EPFL, Lausanne*

<sup>15</sup>*University of Ljubljana, Ljubljana*

<sup>16</sup>*University of Maribor, Maribor*

<sup>17</sup>*University of Melbourne, Victoria*

<sup>18</sup>*Nagoya University, Nagoya*

<sup>19</sup>*Nara Women's University, Nara*

<sup>20</sup>*National Central University, Chung-li*

<sup>21</sup>*National United University, Miao Li*

<sup>22</sup>*Department of Physics, National Taiwan University, Taipei*

<sup>23</sup>*H. Niewodniczanski Institute of Nuclear Physics, Krakow*

<sup>24</sup>*Nippon Dental University, Niigata*

<sup>25</sup>*Niigata University, Niigata*

<sup>26</sup>*Nova Gorica Polytechnic, Nova Gorica*

<sup>27</sup>*Osaka City University, Osaka*

<sup>28</sup>*Osaka University, Osaka*

<sup>29</sup>*Panjab University, Chandigarh*

<sup>30</sup>*Peking University, Beijing*

<sup>31</sup>*Princeton University, Princeton, New Jersey 08544*

<sup>32</sup>*University of Science and Technology of China, Hefei*

<sup>33</sup>*Seoul National University, Seoul*

<sup>34</sup>*Shinshu University, Nagano*

<sup>35</sup>*Sungkyunkwan University, Suwon*

<sup>36</sup>University of Sydney, Sydney NSW

<sup>37</sup>Tata Institute of Fundamental Research, Bombay

<sup>38</sup>Toho University, Funabashi

<sup>39</sup>Tohoku Gakuin University, Tagajo

<sup>40</sup>Tohoku University, Sendai

<sup>41</sup>Department of Physics, University of Tokyo, Tokyo

<sup>42</sup>Tokyo Institute of Technology, Tokyo

<sup>43</sup>Tokyo Metropolitan University, Tokyo

<sup>44</sup>Tokyo University of Agriculture and Technology, Tokyo

<sup>45</sup>University of Tsukuba, Tsukuba

<sup>46</sup>Virginia Polytechnic Institute and State University, Blacksburg, Virginia 24061

<sup>47</sup>Yonsei University, Seoul

(Dated: **February 8, 2020**)

We report the observation of  $B^- \rightarrow J/\psi \Lambda \bar{p}$  and searches for  $B^- \rightarrow J/\psi \Sigma^0 \bar{p}$  and  $B^0 \rightarrow J/\psi p \bar{p}$  decays, using a sample of 275 million  $B\bar{B}$  pairs collected with the Belle detector at the  $\Upsilon(4S)$  resonance. We observe a signal of  $17.2 \pm 4.1$  events with a significance of  $11.1\sigma$  and obtain a branching fraction of  $\mathcal{B}(B^- \rightarrow J/\psi \Lambda \bar{p}) = 11.6 \pm 2.8(\text{stat.})_{-2.3}^{+1.8}(\text{sys.}) \times 10^{-6}$ . No signal is found for either of the two decay modes,  $B^- \rightarrow J/\psi \Sigma^0 \bar{p}$  and  $B^0 \rightarrow J/\psi p \bar{p}$ , and upper limits for the branching fractions are determined to be  $\mathcal{B}(B^- \rightarrow J/\psi \Sigma^0 \bar{p}) < 1.1 \times 10^{-5}$  and  $\mathcal{B}(B^0 \rightarrow J/\psi p \bar{p}) < 8.3 \times 10^{-7}$  at 90% confidence level.

PACS numbers: 13.25.Hw, 14.40.Gx, 14.40.Nd

We report the observation of the decay mode  $B^- \rightarrow J/\psi \Lambda \bar{p}$ , which is a new type of baryonic  $B$  decay,  $B \rightarrow \text{charmonium} + \text{baryons}$ . Evidence for this mode was reported in previous studies by BaBar [1] and Belle [2], with 89 million and 85 million  $B\bar{B}$  pairs, respectively.

Originally, these modes were proposed as a potential explanation [3] for the excess in the low momentum region of the inclusive  $J/\psi$  momentum spectrum for  $B \rightarrow J/\psi + X$  [4, 5], which is not consistent with the predictions from nonrelativistic QCD calculations [6]. Although the measured branching fraction,  $\mathcal{O}(10^{-5})$ , is not big enough to explain the observed excess, this result stimulated experiments to explore new baryonic  $B$  decay modes in addition to those that had already been observed, namely:  $B \rightarrow \text{charmed baryon} (+ \text{light mesons})$  [7],  $B \rightarrow D + \text{baryons}$  [8],  $B \rightarrow \text{charmless baryons} + \text{light mesons}$  [9], and  $B \rightarrow \text{baryons} + \gamma$  [10]. One of the interesting universal features of three-body baryonic  $B$  decays is the presence of an enhancement in the threshold region of the baryon anti-baryon invariant mass spectrum. Further studies of  $B \rightarrow J/\psi \Lambda \bar{p}$  and related baryonic decay modes are expected to provide some additional information on the baryon formation mechanism in  $B$  decays.

In this paper, we report the observation of  $B^- \rightarrow J/\psi \Lambda \bar{p}$  and searches for  $B^- \rightarrow J/\psi \Sigma^0 \bar{p}$  and  $B^0 \rightarrow J/\psi p \bar{p}$  [11] in a sample of  $253 \text{ fb}^{-1}$  containing 275 million  $B\bar{B}$  pairs accumulated at the  $\Upsilon(4S)$  resonance with the Belle detector [12] at the KEKB energy asymmetric  $e^+e^-$  collider [13].

The Belle detector is a large-solid-angle magnetic spectrometer that consists of a silicon vertex detector (SVD), a 50-layer central drift chamber (CDC), an array of aerogel threshold Čerenkov counters (ACC), a barrel-like arrangement of time-of-flight scintillation counters (TOF),

and an electromagnetic calorimeter comprised of CsI(Tl) crystals (ECL). These detectors are located inside a superconducting solenoid coil that provides a 1.5 T magnetic field. An iron flux-return located outside of the coil is instrumented to detect  $K_L$  mesons and to identify muons (KLM).

Candidates for  $B^- \rightarrow J/\psi \Lambda \bar{p}$  and  $B^0 \rightarrow J/\psi p \bar{p}$  are fully reconstructed with all daughters in the final states, where we use the decay chains  $J/\psi \rightarrow l^+l^-$  ( $l = e, \mu$ ) and  $\Lambda \rightarrow p\pi^-$ . Candidates for  $B^- \rightarrow J/\psi \Sigma^0 \bar{p}$  are reconstructed partially, where only the daughters from the  $J/\psi$  and  $\Lambda$  decays plus the anti-proton are reconstructed in the final state. The  $\Lambda$  originates from the  $\Sigma^0 \rightarrow \Lambda\gamma$  decay. Partial reconstruction of  $B^- \rightarrow J/\psi \Sigma^0 \bar{p}$  without the low momentum  $\gamma$  from the  $\Sigma^0$  decay gives better sensitivity than full reconstruction because of the low detection efficiency for soft photons. As a result, the same selection criteria are applied for fully reconstructed  $B^- \rightarrow J/\psi \Lambda \bar{p}$  and partially reconstructed  $B^- \rightarrow J/\psi \Sigma^0 \bar{p}$ .

Events are required to pass a basic hadronic event selection [14]. To suppress continuum background ( $e^+e^- \rightarrow q\bar{q}$ , where  $q = u, d, s, c$ ), we require the ratio of the second to zeroth Fox-Wolfman moments [15] to be less than 0.5.

The selection criteria for the  $J/\psi$  decaying to  $l^+l^-$  are identical to those used in our previous papers [2, 14].  $J/\psi$  candidates are pairs of oppositely charged tracks that originate from within 5 cm of the nominal interaction point (IP) along the beam direction and are positively identified as leptons. In order to reduce the effect of bremsstrahlung or final state radiation, photons detected in the ECL within 0.05 radians of the original  $e^-$  or  $e^+$  direction are included in the calculation of the  $e^+e^-(\gamma)$  invariant mass. Because of the radiative low-

mass tail, the  $J/\psi$  candidates are required to be within an asymmetric invariant mass window:  $-150(-60) \text{ MeV}/c^2 < M_{e^+e^-(\gamma)}(M_{\mu^+\mu^-}) - m_{J/\psi} < +36(+36) \text{ MeV}/c^2$ , where  $m_{J/\psi}$  is the nominal  $J/\psi$  mass [16]. In order to improve the momentum resolution of the  $J/\psi$  signal, a vertex and mass constraint fit to the reconstructed  $J/\psi$  candidates is then performed and a loose cut on the vertex fit quality is applied.

In order to identify hadrons, a likelihood  $L_i$  for each hadron type  $i$  ( $i = \pi, K$  and  $p$ ) is formed using information from the ACC, TOF and  $dE/dx$ . Charged tracks that were previously identified as electrons or muons are rejected in the hadron identification procedure. The proton and pion from the  $\Lambda$  decay are selected with the requirements of  $L_p/(L_p + L_K) > 0.6$  and  $L_\pi/(L_\pi + L_K) > 0.6$ , which have efficiencies of 94.8% and 99.2%, respectively.

The primary protons from the  $B^-$  ( $B^0$ ) decay are selected with requirements of  $L_p/(L_p + L_K) > 0.6$  (0.7) and  $L_p/(L_p + L_\pi) > 0.9$  (0.9). For the primary proton, we also apply requirements on  $dr$  and  $dz$ , the impact parameters perpendicular to and along the beam direction with respect to the IP, respectively.

For  $\Lambda$  candidates, we impose momentum-dependent requirements on the  $dr$  values for both  $\Lambda$  daughter tracks, the distance between the daughter tracks along the beam axis at the  $\Lambda$  vertex, the difference of azimuthal angles between the  $\Lambda$  momentum and the direction of the  $\Lambda$  vertex from the IP, and the flight length of the  $\Lambda$ . The invariant mass of the  $\Lambda$  candidate is required to be within  $5 \text{ MeV}/c^2$  ( $3\sigma$ ) of the  $\Lambda$  mass. We apply vertex and mass constrained fits for the  $\Lambda$  candidates to improve the momentum resolution.

$B$  mesons are reconstructed by combining a  $J/\psi$ , a  $\Lambda(p)$  and a  $\bar{p}$  candidate. To reduce combinatorial background, we impose a requirement on the quality ( $\chi^2$ ) of the vertex fit for the leptons from  $J/\psi$  and primary protons that retains 95.8% (95.1%) of  $B^-$  ( $B^0$ ) signal.

These criteria maximize  $N_{\text{sig}}/\sqrt{N_{\text{sig}} + N_{\text{bkg}}}$ , where  $N_{\text{sig}}$  is the number of expected signal events from signal Monte Carlo (MC) samples with assumed branching fractions of  $1.0 \times 10^{-5}$  for  $B^- \rightarrow J/\psi \Lambda \bar{p}$  and  $1.0 \times 10^{-6}$  for  $B^0 \rightarrow J/\psi p \bar{p}$ , and  $N_{\text{bkg}}$  is the number of expected background events estimated from the sideband data.

We identify  $B$  candidates using two kinematic variables calculated in the center-of-mass system: the beam-energy constrained mass ( $M_{\text{bc}} \equiv \sqrt{E_{\text{beam}}^2 - P_B^2}$ ) and the mass difference ( $\Delta M_B \equiv M_B - m_B$ ) [17], where  $E_{\text{beam}}$  is the beam energy,  $P_B$  and  $M_B$  are the reconstructed momentum and mass of the  $B$  candidate, and  $m_B$  is the nominal  $B$  mass.  $B^-$  ( $B^0$ ) candidates within  $|\Delta M_B| < 0.20 \text{ GeV}/c^2$  ( $-0.32 \text{ GeV}/c^2 < \Delta M_B < 0.20 \text{ GeV}/c^2$ ) and  $M_{\text{bc}} > 5.20 \text{ GeV}/c^2$  are selected for the final analysis. The signal regions are defined to be  $5.27 \text{ GeV}/c^2 < M_{\text{bc}} < 5.29 \text{ GeV}/c^2$  and  $|\Delta M_B| < 0.03 \text{ GeV}/c^2$  for  $B^- \rightarrow J/\psi \Lambda \bar{p}$ ,  $5.265 \text{ GeV}/c^2 < M_{\text{bc}} < 5.29 \text{ GeV}/c^2$

and  $-0.104 \text{ GeV}/c^2 < \Delta M_B < -0.044 \text{ GeV}/c^2$  for partially reconstructed  $B^- \rightarrow J/\psi \Sigma^0 \bar{p}$ , and  $5.27 \text{ GeV}/c^2 < M_{\text{bc}} < 5.29 \text{ GeV}/c^2$  and  $|\Delta M_B| < 0.02 \text{ GeV}/c^2$  for  $B^0 \rightarrow J/\psi p \bar{p}$ , which corresponds to three standard deviations based on the MC simulation. The candidates outside of the signal region are used to study background.

After all selection requirements, about 11% of the  $B^- \rightarrow J/\psi \Lambda \bar{p}$  candidates have more than one entry per event; this occurs for 20% of the partially reconstructed  $B^- \rightarrow J/\psi \Sigma^0 \bar{p}$  and 3.8% of the  $B^0 \rightarrow J/\psi p \bar{p}$  candidates. For these events, the  $B$  candidate with the best vertex quality is used. If an event satisfies both  $B^- \rightarrow J/\psi \Lambda \bar{p}$  and  $B^0 \rightarrow J/\psi p \bar{p}$  selection criteria, we select the  $B^- \rightarrow J/\psi \Lambda \bar{p}$  candidate.

The signal yields are extracted by maximizing the two dimensional (2D) extended likelihood function,

$$\mathcal{L} = \frac{e^{-\sum_k N_k}}{N!} \prod_{i=1}^N \left[ \sum_k N_k \times P_k(M_{\text{bc}}^i, \Delta M_B^i) \right],$$

where  $N$  is the total number of candidate events,  $i$  is the identifier of the  $i$ -th event,  $N_k$  and  $P_k$  are the yield and probability density function (PDF) of the component  $k$ , which corresponds to the signal and background. The  $B^- \rightarrow J/\psi \Lambda \bar{p}$  and partially reconstructed  $B^- \rightarrow J/\psi \Sigma^0 \bar{p}$  samples are fitted simultaneously.

The signal PDFs for all three decay modes are modeled using a sum of two Gaussians for  $M_{\text{bc}}$  and a sum of two Gaussians plus a bifurcated Gaussian that describes the tail of the distribution for  $\Delta M_B$ . The PDF parameters are initially determined using signal MC and subsequently the primary Gaussian parameters are corrected using a control data sample of  $B^+ \rightarrow J/\psi K^{*+}$  ( $K^{*+} \rightarrow K_s \pi^+$ ). The parameters are kept fixed in the fits to the data.

The dominant background comes from random combinations of  $J/\psi$ ,  $\Lambda$  ( $p$ ), and  $\bar{p}$  candidates. A threshold function [18] is used for the  $M_{\text{bc}}$  PDF. For  $\Delta M_B$ , we take the effect of the kinematic boundary into account by using the function

$$P_{\text{thr}}(x; x_c, p, c) = \begin{cases} (x - x_c)^p e^{-c(x - x_c)} & (x \geq x_c) \\ 0 & (x < x_c) \end{cases}$$

with  $x = \Delta M_B$  and  $x_c = -(m_B - m_{J/\psi} - m_\Lambda(m_p) - m_{\bar{p}})$ , where  $m_B$ ,  $m_{J/\psi}$ ,  $m_\Lambda$  ( $m_p$ ) and  $m_{\bar{p}}$  are the nominal masses of the  $B$ ,  $J/\psi$ ,  $\Lambda$  ( $p$ ) and  $\bar{p}$ , respectively.

For  $B^0 \rightarrow J/\psi p \bar{p}$ , a cross-feed from  $B^- \rightarrow J/\psi \Lambda \bar{p}$ , where the  $\pi$  from the  $\Lambda$  is undetected, forms a peak in the negative  $\Delta M_B$  sideband region. The PDF for this cross-feed is modeled by a smoothed histogram from the  $B^- \rightarrow J/\psi \Lambda \bar{p}$  MC sample.

In the fit, the value of  $N_k$  and the parameters for combinatoric background are allowed to float. Figures 1 and 2 show the  $(M_{\text{bc}}, \Delta M_B)$  scatterplots and their projections for candidates after all selections are applied. The

TABLE I: Summary of the results.  $Y$  and  $b$  are the signal and expected total background yields in the signal region,  $n_0$  is the observed number of candidate events in the signal region,  $\epsilon$  (error includes systematic error) is the detection efficiency,  $Y_{90}$  is the upper limit on the signal yield at 90% confidence level and  $\mathcal{B}$  is the branching fraction.

mode	$Y$	$b$	$n_0$	$\epsilon(\%)$	$Y_{90}$	$\mathcal{B}$
$B^- \rightarrow J/\psi \Lambda \bar{p}$	$17.2 \pm 4.1$	$0.41 \pm 0.09(\text{stat.})$	16	$7.2^{+1.1}_{-1.4}$	—	$11.6 \pm 2.8(\text{stat.})^{+1.8}_{-2.3}(\text{sys.}) \times 10^{-6}$
$B^- \rightarrow J/\psi \Sigma^0 \bar{p}$	$-1.1 \pm 1.7$	$0.31 \pm 0.04(\text{stat.}) \pm 0.03(\text{sys.})$	1	$2.3^{+0.9}_{-0.8}$	$< 5.3$	$< 1.1 \times 10^{-5}$
$B^0 \rightarrow J/\psi p \bar{p}$	$-6.1 \pm 2.2$	$0.94 \pm 0.10(\text{stat.})^{+0.04}_{-0.16}(\text{sys.})$	3	$26.4^{+6.8}_{-5.4}$	$< 7.1$	$< 8.3 \times 10^{-7}$

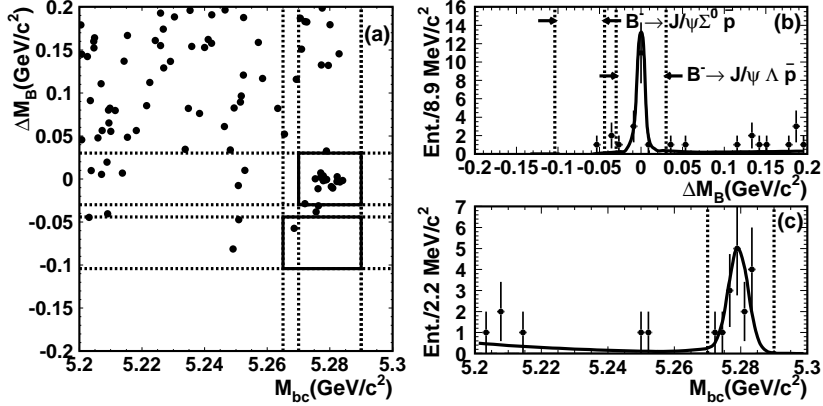


FIG. 1: (a) The  $(M_{bc}, \Delta M_B)$  scatterplot of  $B^- \rightarrow J/\psi \Lambda \bar{p}$  candidates and its projections onto (b)  $\Delta M_B$  with  $5.265 \text{ GeV}/c^2 < M_{bc} < 5.29 \text{ GeV}/c^2$  and (c)  $M_{bc}$  with  $|\Delta M_B| < 0.03 \text{ GeV}/c^2$ . The dashed lines and solid boxes indicate the signal regions. The curves are the result of the fit as described in the text.

fit results are superimposed on the projections. There are sixteen candidate events in the signal region for  $B^- \rightarrow J/\psi \Lambda \bar{p}$ , one for  $B^- \rightarrow J/\psi \Sigma^0 \bar{p}$  and three for  $B^0 \rightarrow J/\psi p \bar{p}$ .

Table I summarizes the maximum-likelihood fit results for the signal ( $Y$ ) and signal-region background ( $b$ ) yields and their statistical errors. For the  $B^- \rightarrow J/\psi \Lambda \bar{p}$  decay the fit gives  $17.2 \pm 4.1$  signal events with a statistical significance of  $11.1\sigma$ . The statistical significance is defined as  $\sqrt{-2\ln(\mathcal{L}_0/\mathcal{L}_{\max})}$ , where  $\mathcal{L}_{\max}$  and  $\mathcal{L}_0$  denote the maximum likelihood with the fitted signal yield and with the yield fixed at zero, respectively. No significant signal is found for the  $B^- \rightarrow J/\psi \Sigma^0 \bar{p}$  and  $B^0 \rightarrow J/\psi p \bar{p}$  decay modes, while the number of cross-feed events in the  $\Delta M_B$  sideband of  $B^0 \rightarrow J/\psi p \bar{p}$  ( $9.0 \pm 3.2$ ) is consistent with the expectation from the observed  $B^- \rightarrow J/\psi \Lambda \bar{p}$  signal yield ( $7.0 \pm 1.7$ ). For these two modes, we obtain upper limits on the yield at 90% confidence level ( $Y_{90}$ ) using the Feldman-Cousins method [19], which takes into account the systematic errors due to the uncertainties in the signal detection efficiency and the background yield [20].

The branching fraction is determined with  $N_S/[\epsilon \times N_{B\bar{B}} \times \mathcal{B}(J/\psi \rightarrow l^+ l^-) \times \mathcal{B}(\Lambda \rightarrow p \pi^-)]$  for  $B^- \rightarrow J/\psi \Lambda \bar{p}$  and the partially reconstructed  $B^- \rightarrow J/\psi \Sigma^0 \bar{p}$ . For  $B^0 \rightarrow J/\psi p \bar{p}$  we use  $N_S/[\epsilon \times N_{B\bar{B}} \times \mathcal{B}(J/\psi \rightarrow l^+ l^-)]$ . Here  $N_S$  is the signal yield,  $N_{B\bar{B}}$  is the number of  $B\bar{B}$  pairs. We use the world averages [16] for the branching

fractions of  $\mathcal{B}(J/\psi \rightarrow l^+ l^-)$  and  $\mathcal{B}(\Lambda \rightarrow p \pi^-)$ . The efficiencies ( $\epsilon$ ) are determined from the signal MC sample with the same selection as used in the data. A three-body phase space model is employed for all three decay modes. The fractions of neutral and charged  $B$  mesons produced in  $\Upsilon(4S)$  decays are assumed to be equal.

Figure 3 demonstrates the consistency between the observed invariant mass distributions  $M(J/\psi \Lambda)$ ,  $M(J/\psi \bar{p})$ , and  $M(\Lambda \bar{p})$  of the sixteen  $B^- \rightarrow J/\psi \Lambda \bar{p}$  candidates and the phase space distributions obtained from signal MC.

The sources and sizes of systematic uncertainties are summarized in Table II. The systematic uncertainty on the yield is examined by varying each fixed shape parameter by  $\pm 1\sigma$ . A possible bias in the fitting is studied using MC samples; no significant bias is found. The systematic uncertainty assigned to the yield is 2.5%.

The dominant sources of systematic errors on the efficiency are uncertainties in the three-body decay model,  $\Lambda$  reconstruction, tracking efficiency and particle identification. To estimate the error due to uncertainty in decay modeling for  $B^- \rightarrow J/\psi \Lambda \bar{p}$ , we subdivide phase space into a few bins and recompute the branching fraction using MC-determined bin-by-bin efficiencies. The maximum difference between the nominal value of the branching fraction and the values obtained with different choices of bins is assigned as a systematic error. For  $B^- \rightarrow J/\psi \Sigma^0 \bar{p}$  ( $B^0 \rightarrow J/\psi p \bar{p}$ ), the distribution in phase space is unknown and we conservatively assign

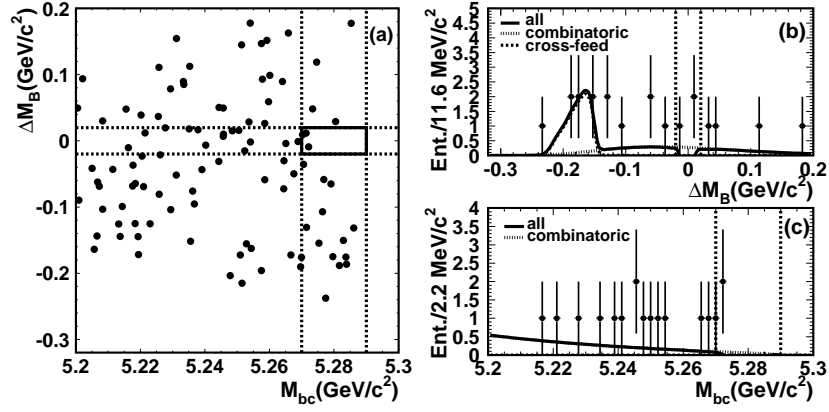


FIG. 2: (a)  $(M_{bc}, \Delta M_B)$  scatterplot of  $B^0 \rightarrow J/\psi p \bar{p}$  candidates and its projections on to (b)  $\Delta M_B$  with  $5.27 \text{ GeV}/c^2 < M_{bc} < 5.29 \text{ GeV}/c^2$  and (c)  $M_{bc}$  with  $|\Delta M_B| < 0.02 \text{ GeV}/c^2$ . The dashed lines and the solid box indicate the signal regions. The curves are the result of the fit.

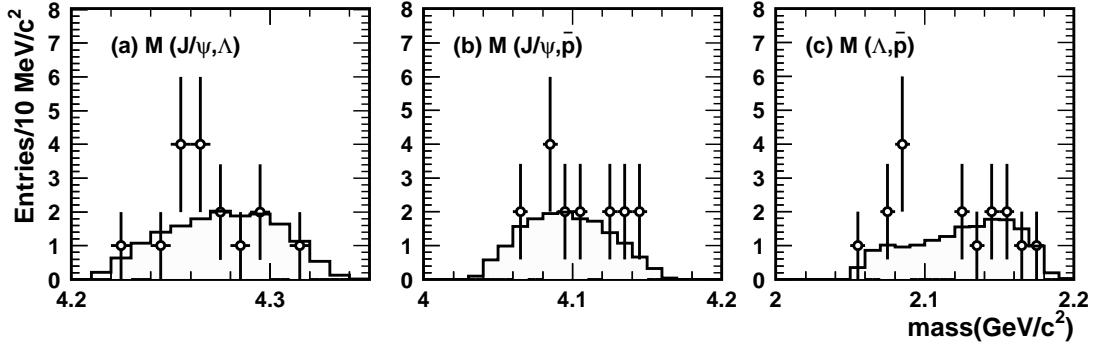


FIG. 3: Invariant mass distributions for (a)  $M(J/\psi\Lambda)$ , (b)  $M(J/\psi\bar{p})$  and (c)  $M(\Lambda\bar{p})$  for the sixteen signal-region  $B^- \rightarrow J/\psi\Lambda\bar{p}$  candidates. The histograms are phase space distributions from the signal MC sample normalized to sixteen events.

the maximum variation of efficiency among the slices of  $M(J/\psi, \Lambda)$ ,  $M(J/\psi, \bar{p})$  and  $M(\Lambda, \bar{p})$  [ $M(J/\psi, p)$ ,  $M(J/\psi, \bar{p})$  and  $M(p, \bar{p})$ ] as a systematic uncertainty. The  $\Lambda$  reconstruction error is determined by comparing the transverse proper flight distance distributions for data and MC simulation. The discrepancies weighted by distributions of the  $\Lambda$  momentum and the decay length are assigned as systematic errors. The uncertainties in the tracking efficiency are estimated by linearly adding the momentum-dependent single track systematic errors. We assign uncertainties of 3% per proton, 2% per pion, and 2% per lepton for the particle and lepton identification.

The systematic errors for the background yield are evaluated by varying each of the PDF parameters by its statistical error from the fit and by fixing the signal yield at zero in the case of  $B^0 \rightarrow J/\psi p \bar{p}$  to accommodate the possibility that an overestimate of the background might be causing the large negative signal yield  $(-6.1 \pm 2.2)$ .

In summary, we have observed a  $17.2 \pm 4.1$  event signal for  $B^- \rightarrow J/\psi\Lambda\bar{p}$ , with a statistical significance of  $11.1\sigma$ . The measured branching fraction is  $\mathcal{B}(B^- \rightarrow J/\psi\Lambda\bar{p}) = 11.6 \pm 2.8(\text{stat.})_{-2.3}^{+1.8}(\text{sys.}) \times 10^{-6}$ . This establishes a new type of baryonic  $B$  decay,  $B \rightarrow \text{charmonium} +$

baryon anti-baryon. The  $\Lambda\bar{p}$  distribution for this decay is consistent with a phase space, in contrast to  $B \rightarrow \Lambda\bar{p}\pi$  [9] and other baryonic  $B$  decays. No significant signals are found for the  $B^- \rightarrow J/\psi\Sigma^0\bar{p}$  and  $B^0 \rightarrow J/\psi p \bar{p}$  decay modes. We obtain upper limits on the branching fractions of  $\mathcal{B}(B^- \rightarrow J/\psi\Sigma^0\bar{p}) < 1.1 \times 10^{-5}$  and  $\mathcal{B}(B^0 \rightarrow J/\psi p \bar{p}) < 8.3 \times 10^{-7}$  at 90% confidence level.

We thank the KEKB group for the excellent operation of the accelerator, the KEK cryogenics group for the efficient operation of the solenoid, and the KEK computer group and the NII for valuable computing and Super-SINET network support. We acknowledge support from MEXT and JSPS (Japan); ARC and DEST (Australia); NSFC (contract No. 10175071, China); DST (India); the BK21 program of MOEHRD, and the CHEP SRC and BR (grant No. R01-2005-000-10089-0) programs of KOSEF (Korea); KBN (contract No. 2P03B 01324, Poland); MIST (Russia); MHEST (Slovenia); SNSF (Switzerland); NSC and MOE (Taiwan); and DOE (USA).

TABLE II: Summary of systematic uncertainties (%) in yield and detection efficiency.

Source	$B^- \rightarrow J/\psi \Lambda \bar{p}$	$B^- \rightarrow J/\psi \Sigma^0 \bar{p}$	$B^0 \rightarrow J/\psi p \bar{p}$
Uncertainty in yield	$\pm 2.5$	-	-
Tracking Error	$\pm 8.6$	$\pm 9.8$	$\pm 4.8$
PID(proton and pion)	$\pm 8.0$	$\pm 8.0$	$\pm 6.0$
Lepton ID	$\pm 4.0$	$\pm 4.0$	$\pm 4.0$
$\Lambda$ Reconstruction	$\pm 7.9$	$\pm 9.8$	-
$\Lambda$ BR	$\pm 0.8$	$\pm 0.8$	-
MC Statistics	$\pm 0.2$	$\pm 0.2$	$\pm 0.5$
3-body decay model	$+4.7/-12.6$	$+38.0/-29.1$	$+24.1/-18.8$
Total	$+15.7/-19.6$	$+41.4/-33.4$	$+25.6/-20.7$

- 
- [1] Babar Collaboration, B. Aubert *et al.*, Phys. Rev. Lett. **90**, 231801 (2003).
- [2] Belle Collaboration, S.L. Zang *et al.*, Phys. Rev. D **69**, 017101 (2004).
- [3] S.J. Brodsky and F.S. Navarra, Phys. Lett. B **411**, 152 (1997).
- [4] CLEO Collaboration, R. Balest *et al.*, Phys. Rev. D **52**, 2661(1995); S. Anderson *et al.*, Phys. Rev. Lett. **89**, 282001 (2003).
- [5] Babar Collaboration, B. Aubert *et al.*, Phys. Rev. D **67**, 032002 (2003).
- [6] M. Beneke, G.A. Schuler, and S. Wolf, Phys. Rev. D **62**, 034004 (2003).
- [7] CLEO Collaboration, X. Fu *et al.*, Phys. Rev. Lett. **79**, 3125 (1997); Belle Collaboration, N. Gabyshev *et al.*, Phys. Rev. D **66**, 091102(R) (2002); Belle Collaboration, N. Gabyshev *et al.*, Phys. Rev. Lett. **90**, 121802 (2003);
- [8] CLEO Collaboration, S. Anderson *et al.*, Phys. Rev. Lett. **86**, 2732 (2001); Belle Collaboration, K. Abe *et al.*, Phys. Rev. Lett. **89**, 151802 (2002).
- [9] Belle Collaboration, K. Abe *et al.*, Phys. Rev. Lett. **88**, 181803 (2002); Belle Collaboration, M.Z. Wang *et al.*, Phys. Rev. Lett. **90**, 201802 (2003); Belle Collaboration, M.Z. Wang *et al.*, Phys. Rev. Lett. **92**, 131801 (2003); Belle Collaboration, Y.J. Lee *et al.*, Phys. Rev. Lett. **93**, 211801 (2004).
- [10] Belle Collaboration, Y.J. Lee *et al.*, hep-ex/0503046.
- [11] Inclusion of the charge conjugate state is implied throughout this paper.
- [12] Belle Collaboration, A. Abashian *et al.*, Nucl. Instr. and Meth. A **479**, 117 (2002).
- [13] S. Kurokawa and E. Kikutani, Nucl. Instr. and Meth. A **499**, 1 (2003).
- [14] Belle Collaboration, K. Abe *et al.*, Phys. Rev. D **67**, 032003 (2003).
- [15] G.C. Fox and S. Wolfram, Phys. Rev. Lett. **41**, 1581 (1978).
- [16] S. Eidelman *et al.* (Particle Data Group), Phys. Lett. B **592**, 1 (2004).
- [17] The benefit of using of  $\Delta M_B$  instead of the energy difference is described in Ref [2].
- [18] ARGUS Collaboration, H. Albrecht *et al.*, Phys. Lett. B **241**, 278 (1990).
- [19] G.J. Feldman and R.D. Cousins, Phys. Rev. D **57**, 3873 (1998).
- [20] J. Conrad *et al.*, Phys. Rev. D **67**, 012002 (2003).